Insulator, metal, or superconductor: The criteria

Douglas J. Scalapino
Department of Physics, University of California, Santa Barbara, California 93106-9530

Steven R. White
Department of Physics, University of California, Irvine, California 92717

Shoucheng Zhang
IBM Research Division, Almaden Research Center, San Jose, California 95120-6099

(Received 4 August 1992; revised manuscript received 16 November 1992)

The appropriate infinite-wavelength $q_i \rightarrow 0$ and zero-frequency $\omega \rightarrow 0$ limits of the paramagnetic current-current correlation function provide criteria for determining whether a system is insulating, metallic, or superconducting. Here we discuss these criteria for lattice models and present Monte Carlo data for the two-dimensional positive- and negative-U Hubbard models that imply that the ground state of the half-filled positive-U Hubbard model is an insulator, the doped state is a metal, and the negative-U Hubbard model is a superconductor.

I. INTRODUCTION

Given a many-body Hamiltonian, how does one determine whether its ground state is insulating, metallic, or superconducting? With the development of numerical simulation techniques, what has been discussed as a basic question of principle has now become a practical calculational question. For example, one would like to answer this question for the two-dimensional Hubbard model.

One approach has been to study the scaling properties of correlation functions characteristic of the ground-state order one expects.[1] For example, scaling studies of the staggered spin correlations for the two-dimensional half-filled Hubbard model on lattices of increasing size have shown that its ground state has long-range antiferromagnetic order.[2,3] Thus one has, in this way, indirectly concluded that at half-filling the ground state of the two-dimensional Hubbard model is insulating. Away from half-filling, calculations of various types of pair-field correlation functions have so far found only short-range $d_{x^2-y^2}$ and extended s-wave pair-field correlations.[4,5] However, the forms that have been chosen for the pair-field operators have described a short-range equal-time pair constructed using bare fermion operators. It is possible that one needs dressed operators to get a sizeable response[6] or, worse yet, that the pair-field operators that have been examined have the wrong symmetry. Perhaps the system would be found to have clear superconducting correlations if the physically correct pair-field operator had been guessed. Thus, as a practical matter, one would like to know what to calculate in order to determine if the ground state of a system is insulating, metallic, or superconducting. Beyond this, theoretical questions associated with the nature of the metal-insulator and superconducting-insulator transition require a clear understanding of the relevant criteria.

In a previous paper,[7] we have suggested that the appropriate $q_i \rightarrow 0$ and $\omega \rightarrow 0$ limits of the current response kernel provide the framework for answering this question. Here, in Sec. II we review this approach and introduce a Drude weight $D/\pi e^2$, which is a measure of the ratio of the density of the mobile charge carriers to their mass and a superfluid weight $D_s/\pi e^2$, which measures the ratio of the superfluid density to mass. The superfluid weight, unlike the pair-correlation function, is a physical quantity directly measurable in experiments. Therefore, this method yields a criterion for superconductivity independent of the nature of the order parameter. Some mean-field examples are discussed in Sec. III. Following this, in Sec. IV we discuss the relationship of this approach to the energy shift of the ground state with respect to twisted boundary conditions. In Sec. V we show that when there is a gap, $D_s = D$. Then in Sec. VI, results from Monte Carlo calculations on the Hubbard model are discussed. Section VII contains a summary and our conclusions.

II. THE DRUDE AND SUPERFLUID WEIGHTS

The model Hamiltonians which we will study have a kinetic energy

$$K = -t \sum_{\langle ij \rangle s} (c_{is}^{\dagger} c_{js} + c_{js}^{\dagger} c_{is}) \ . \tag{1}$$

Here t is a one-electron overlap between near-neighbor sites on a square lattice, and $c_{is}^{\dagger}$ creates an electron of spin s on site i. The interaction can have, for example, an on-site $Un_{i\uparrow}n_{i\downarrow}$ or extended Vn_in_j Hubbard form or involve an electron-photon coupling gn_ix_i in which the site energy depends on a lattice displacement x_i. Here we are interested in the current response to a vector potential $A_x(l,t)$. In the presence of a vector potential, the hopping term $c_{l+x}^{\dagger} c_{ls}$ is modified[8] by the phase factor $e^{ieA_x(l)}$. Here and in the following we will set $\hbar = c = 1$ and take the lattice spacing equal to 1. Expanding the phase factors in the usual manner through terms

of order A^2, one has

$$K_A = K - \sum_l \left[e j_x^P(l) A_x(l) + \frac{e^2 k_x(l)}{2} A_x^2(l) \right] . \quad (2)$$

Here $e j_x^P$ is the x component of the paramagnetic current density

$$j_x^P(l) = it \sum_s (c_{l+xs}^\dagger c_{ls} - c_{ls}^\dagger c_{l+xs}) , \quad (3)$$

and $k_x(l)$ is the kinetic-energy density associated with the x-oriented links

$$k_x(l) = -t \sum_s (c_{l+xs}^\dagger c_{ls} + c_{ls}^\dagger c_{l+xs}) . \quad (4)$$

The total current-density $j_x(l)$ is obtained by differentiating Eq. (2) with respect to $A_x(l)$,

$$j_x(l) = -\frac{\delta K}{\delta A_x(l)} = e j_x^P(l) + e^2 k_x(l) A_x(l) \quad (5)$$

and consists of the usual paramagnetic and diamagnetic parts.

For a vector potential

$$A_x(l,t) = \mathrm{Re}(A_x(\mathbf{q},\omega) e^{i\mathbf{q}\cdot\mathbf{l} - i\omega t}) \quad (6)$$

the current response is

$$\langle j_x(l,t) \rangle = \mathrm{Re}(\langle j_x(\mathbf{q},\omega) \rangle e^{i\mathbf{q}\cdot\mathbf{l} - i\omega t}) , \quad (7)$$

with

$$\langle j_x(\mathbf{q},\omega) \rangle = -e^2 [\langle -k_x \rangle - \Lambda_{xx}(\mathbf{q},\omega)] A_x(\mathbf{q},\omega) . \quad (8)$$

Here $\langle k_x \rangle$ is the kinetic energy per site divided by the number of lattice dimensions. $\Lambda_{xx}(\mathbf{q},\omega)$ is obtained from

$$\Lambda_{xx}(\mathbf{q}, i\omega_m) = \frac{1}{N} \int_0^\beta d\tau \, e^{i\omega_m \tau} \langle j_x^P(\mathbf{q},\tau) j_x^P(-\mathbf{q},0) \rangle , \quad (9)$$

with $\omega_m = 2\pi m T$, by the usual analytic continuation in which $\omega_m \to \omega + i\delta$, and

$$j_x^P(\mathbf{q}) = it \sum_l e^{-i\mathbf{q}\cdot\mathbf{l}} (c_{l+xs}^\dagger c_{ls} - c_{ls}^\dagger c_{l+xs}) . \quad (10)$$

The long-wavelength $\mathbf{q} \to 0$ and low-frequency $\omega \to 0$ limits of the Kubo linear response relations, Eq. (8), determine whether a system is insulating, metallic, or superconducting. We begin by examining the criteria for superconductivity.[9,10] London[11] showed that the Meissner effect followed if the current-density response of a superconductor in a static, $\omega = 0$, long wavelength $q_y \to 0$, transverse $\mathbf{q}\cdot\mathbf{A} = 0$ vector potential was given by

$$j_x(q_y) = -\frac{1}{4\pi} \frac{1}{\lambda^2} A_x(q_y) . \quad (11)$$

In this case, the magnetic field would be expelled except for a penetration depth λ, with

$$\frac{1}{\lambda^2} = \frac{4\pi n_s e^2}{mc^2} . \quad (12)$$

Here n_s is the superfluid density and m the electron mass. In general, for a static $\omega = 0$ vector potential, in the long-wavelength limit one has

$$\langle j_i(\mathbf{q}) \rangle = f(\mathbf{q}) \left[\delta_{ij} - \frac{q_i q_j}{\mathbf{q}^2} \right] A_j(\mathbf{q}) . \quad (13)$$

For a superconductor,

$$\frac{-f(\mathbf{q} \to \mathbf{0})}{e^2} = \left[\frac{n_s}{m} \right]^* \equiv \frac{D_s}{\pi e^2} , \quad (14)$$

where we have introduced a superfluid weight D_s which measures the ratio of the superfluid density to the mass. Now, from the linear response relation, Eq. (8), and Eqs. (13) and (14), we have

$$\frac{D_s}{\pi e^2} = \langle -k_x \rangle - \Lambda_{xx}(q_x = 0, \; q_y \to 0, \; i\omega_m = 0) \quad (15)$$

and

$$0 = \langle -k_x \rangle - \Lambda_{xx}(q_x \to 0, \; q_y = 0, \; i\omega_m = 0) . \quad (16)$$

The fact that the static paramagnetic current-current correlation function $\Lambda_{xx}(\mathbf{q}, \omega_m = \mathbf{0})$ approaches different limits depending upon the order in which q_x and q_y go to zero implies that the paramagnetic current-current correlations in a superconductor are long range.[10,12] In three dimensions they decay as r^{-3} and in two dimensions as r^{-2}.

The $\mathbf{q} = \mathbf{0}$, $\omega \to 0$ limit of the conductivity determines whether the ground state of a system has zero resistance. Consider the $\tau \to \infty$ limit of the real part of the Drude conductivity

$$\sigma_1(\omega) = \lim_{\tau \to \infty} \frac{e^2 n \tau}{m} \frac{1}{1 + (\omega\tau)^2} = D\delta(\omega) . \quad (17)$$

The coefficient D of the delta function is called the Drude weight, and the simple Drude form is equal to $\pi e^2 n / m$. In general, we expect that at $T = 0$, the real part of the $\mathbf{q} = \mathbf{0}$ conductivity will have the form

$$\sigma_{xx}(\omega) = D\delta(\omega) + \sigma_{xx}^{\mathrm{reg}}(\omega) , \quad (18)$$

with

$$\frac{D}{\pi e^2} = \left[\frac{n}{m} \right]^* \quad (19)$$

determined by the ratio of the density of the mobile charge carriers to their mass. In the absence of impurities, a metal will be characterized by a finite value of D (i.e., $R = 0$), and an insulator will have a D which vanishes as the size of the system goes to infinity.[13]

Setting $A_x(\mathbf{q} = \mathbf{0}, \omega) = E_x(\mathbf{q} = \mathbf{0}, \omega) / i(\omega + i\delta)$ in Eq. (8), the conductivity for a uniform, $\mathbf{q} = \mathbf{0}$, frequency-dependent electric field is given by

$$\sigma_{xx}(\omega) = -e^2 \frac{\langle -k_x \rangle - \Lambda_{xx}(\mathbf{q} = \mathbf{0}, \omega)}{i(\omega + i\delta)} . \quad (20)$$

In the $\omega \to 0$ limit, the real part of $\sigma_{xx}(\omega)$ will contain a delta function contribution $D\delta(\omega)$ with[13,14]

$$\frac{D}{\pi e^2} = \langle -k_x \rangle - \mathrm{Re}\Lambda_{xx}(q = 0, \; \omega \to 0) . \quad (21)$$

Since Λ_{xx} is analytic in the upper complex plane, we can also obtain D from the zero-temperature extrapolation of the Matsubara form, Eq. (9),

$$\frac{D}{\pi e^2} = \lim_{T\to 0} [-\langle k_x \rangle - \Lambda_{xx}(q=0, i2\pi T)] . \quad (22)$$

Alternatively we will find that at low temperatures, a useful estimate of D can be obtained by extrapolating $i\omega_m \to 0$, using the $m \neq 0$ values

$$\frac{D}{\pi e^2} \cong [-\langle k_x \rangle - \Lambda_{xx}(q=0,\ i\omega_m \to 0)] . \quad (23)$$

In Eqs. (15) and (23) we see that the difference between D_s and D is the order in which q_y and $i\omega_m$ approach zero. The insulating, metallic, or superconducting character of the ground state is determined by the values that D_s and D approach as the size of the system scales to the bulk limit. In this limit, for a system without disorder, we expect that D and D_s go to 0 for an insulator, D is finite and $D_s = 0$ for a metal, and D and D_s are both finite for a superconductor. If there is a gap, whether the system is insulating or superconducting, we expect that $D = D_s$, as discussed in Sec. IV. At finite temperature or if there is disorder, $D = 0$ but $\sigma_{xx}(\omega = 0)$ remains finite for a metallic system.

III. MEAN-FIELD EXAMPLES

In this section, we consider some simple examples in order to develop insight into the limiting behavior of the current-current correlation function. First, for a noninteracting electron system on a two-dimensional square lattice with $\varepsilon_k = -2(\cos k_x + \cos k_y)$, we have for the current-current correlation function

$$\Lambda_{xx}(q_y, \omega_m) = \frac{2}{N} \sum_p \frac{(2\sin p_x)^2 [f(\varepsilon_{p+q_y}) - f(\varepsilon_p)]}{i\omega_m - (\varepsilon_{p+q_y} - \varepsilon_p)} . \quad (24)$$

Here $2\sin p_x$ is the velocity in the x direction, and f is the usual Fermi function. Now, if ω_m is set to zero first and then one takes the limit, q_y goes to zero,

$$\lim_{q_y \to 0} \Lambda_{xx}(q_y, 0) = \frac{-8}{N} \sum_p \sin^2 p_x \frac{\partial f(\varepsilon_p)}{\partial \varepsilon_p} . \quad (25)$$

Carrying out a partial integration, this equals $\langle -k_x \rangle$ so that D_s [Eq. (15)] vanishes, and we conclude that there is no superfluid density in this noninteracting system. In Fig. 1(a), this limiting behavior of $\Lambda_{xx}(q_y \to 0,\ \omega_m = 0)$ is shown and the solid triangle marks $\langle -k_x \rangle$ for $U = 0$.

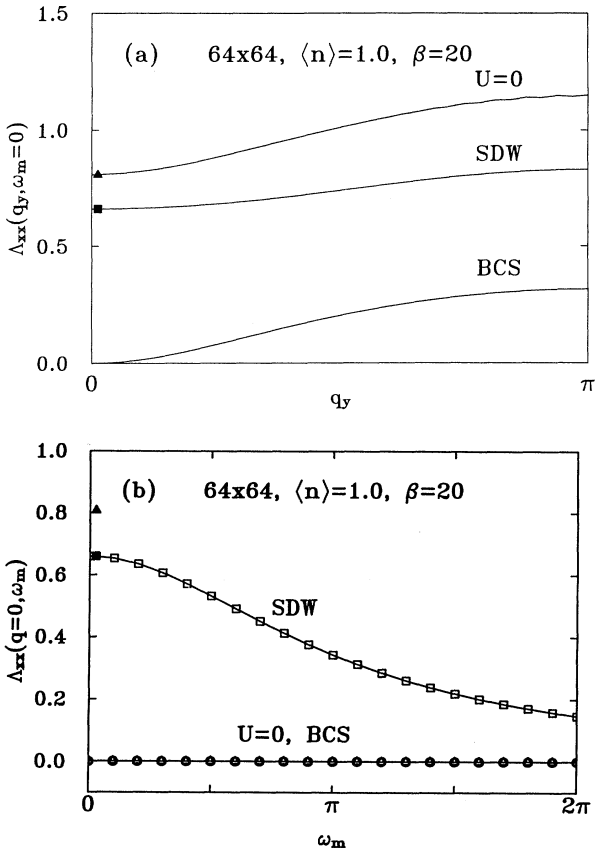

FIG. 1. (a) $\Lambda_{xx}(q_y, \omega_m = 0)$ vs q_y, and (b) $\Lambda_{xx}(\mathbf{q}=\mathbf{0},\ \omega_m)$ vs ω_m for $U = 0$ and mean-field results for $U = 4$ (SDW) and $U = -4$ (BCS) on a 64×64 lattice. Here $\langle n \rangle = 1$ and $\beta = 20$, which correspond to a reduced temperature near zero for the BCS and SDW mean-field solutions. In (a) and (b) the solid triangles mark $\langle -k_x \rangle$ for $U = 0$, while the solid squares mark $\langle -k_x \rangle$ for both the SDW and BCS states. The open symbols in (b) denote the Matsubara frequencies $2\pi m T$ in units of the hopping t.

Certainly this is what one would expect in such a noninteracting fermion system. On the other hand, in the absence of impurities, the $U = 0$ system should have zero resistance. Indeed, for finite ω_m, we see from Eq. (24) that $\Lambda_{xx}(q_y = 0,\ \omega_m \neq 0)$ vanishes, leading to a Drude weight $D/\pi e^2$ equal to $\langle -k_x \rangle$. Thus we conclude that the noninteracting Hubbard model is a metal.

Next consider the BCS mean-field solution of the negative-U Hubbard model. In this case,

$$\Lambda_{xx}(q_y, \omega_m) = \frac{4}{N} \sum_p \sin^2 p_x \left[p^2(p, p+q) \left(\frac{1}{E_p + E_{p+q} + i\omega_m} + \frac{1}{E_p + E_{p+q} - i\omega_m} \right) [1 - f(E_p) - f(E_{p+q})] \right.$$

$$\left. + l^2(p, p+q) \left(\frac{1}{E_p - E_{p+q} + i\omega_m} + \frac{1}{E_p - E_{p+q} - i\omega_m} \right) [f(E_{p+q}) - f(E_p)] \right] , \quad (26)$$

with

$$p^2(p,p+q)=\frac{1}{2}\left[1-\frac{\varepsilon_p\varepsilon_{p+q}+\Delta^2}{E_pE_{p+q}}\right],$$
$$l^2(p,p+q)=\frac{1}{2}\left[1+\frac{\varepsilon_p\varepsilon_{p+q}+\Delta^2}{E_pE_{p+q}}\right], \quad (27)$$

the usual BCS coherence factors.[9] Here $E_p=\sqrt{\varepsilon_p^2+\Delta^2}$, $\varepsilon_p=-2t(\cos p_x+\cos p_y)-\mu$, and Δ is determined from the BCS gap equation. When $\omega_m=0$, the $q_y\to 0$ limit of $\Lambda_{xx}(q_y,0)$ is

$$\Lambda_{xx}(q_y\to 0,0)=-\frac{8}{N}\sum_p \sin^2 p_x \frac{\partial f}{\partial E_p}, \quad (28)$$

which vanishes as $T/T_c\to 0$, as shown in Fig. 1(a). The approach to zero varies as $(q\xi_0)^2$, where ξ_0 is the coherence length $\hbar v_F/\pi\Delta$. The solid square in Fig. 1(a) marks $\langle -k_x\rangle$ for the BCS ground state. In the limit when q_y is first set to zero, $\Lambda_{xx}(0,\omega_m)$ also vanishes, as shown in Fig. 1(b). Thus the superconducting mean-field ground state is characterized by $D_s/\pi e^2=D/\pi e^2=-\langle k_x\rangle$.[15] The BCS mean-field solution, Eq. (26), incorrectly gives $\Lambda_{xx}(q_x\to 0, q_y=0, i\omega_m=0)=0$, violating gauge invariance. However, it is well known[9] that vertex corrections remove this difficulty, and by including them one obtains $\Lambda_{xx}(q_x\to 0, q_y=0, i\omega_m=0)=\langle -k_x\rangle$, restoring gauge invariance.

Another example is the half-filled repulsive-U Hubbard model. In mean-field theory, the low-temperature state has a spin-density wave gap Δ_{SDW}. With this change, Λ_{xx} is given by Eq. (26) with the sign of Δ^2 changed in the numerators of the coherence factors [Eq. (27)], and Δ replaced by the spin-density wave gap Δ_{SDW}. In this case $\Lambda_{xx}(q_y\to 0, \omega_m=0)=-\langle k_x\rangle$, so the superfluid density vanishes. Alternatively, when $q_y=0$ and ω_m goes to zero,

$$\Lambda_{xx}(q_y=0, \omega_m\to 0)=\frac{4}{N}\sum_p \sin^2 p_x \frac{\Delta_{\mathrm{SDW}}^2}{E_p^3}[1-2f(E_p)], \quad (29)$$

and $\Lambda_{xx}(q_y=0, \omega_m\to 0)$ is equal to $-\langle k_x\rangle$ when T goes to zero, as shown in Fig. 1(b). Thus in the mean-field ground state of the half-filled repulsive Hubbard model both D_s and D vanish, consistent with an insulating ground state. Results showing $\Lambda_{xx}(q_x, \omega_m=0)$ vs q_x and $\Lambda_{xx}(q_x=0, \omega_m)$ vs ω_m for this mean-field spin-density wave state at low temperature are shown in Figs. 1(a) and 1(b).

IV. TWISTED BOUNDARY CONDITION

In this section we discuss the relation between the second derivative of the ground-state energy with respect to the flux $\partial^2 E/\partial\phi^2$, the Drude weight D, and the superfluid weight D_s. Kohn[13] was the first to derive an identity between $\partial^2 E/\partial\phi^2$ and D, and it has since been used in calculating the Drude weight for various one-dimensional models.[16,17] It has also been explored for small two-dimensional clusters.[18] However, we would like to point out here that extreme care must be taken in defining these quantities. The Drude weight is obtained from the curvature of a single many-body energy level which is the ground state at $\phi=0$. That is, one must follow this level adiabatically. However, we will argue below that the magnitude of the flux ϕ_c at which another many-body energy level drops below or crosses the $\phi=0$ level varies as

$$\phi_c\sim\left[\frac{hc}{e}\right]\frac{1}{l^{d-1}},$$

where l is the linear sample size and d is the dimension. Thus in the thermodynamic $l\to\infty$ limit, ϕ_c vanishes for $d>1$. In this case, one must take the second derivative of $E(\phi)$ with respect to ϕ first, being certain to calculate the curvature of the adiabatically evolved ground state with twisted boundary conditions, and then let $l\to\infty$ in order to obtain the Drude weight. If, instead, one determines the ground-state energy $E(\phi)$ for $l\to\infty$ and then calculates its second derivative, one obtains the curvature of the envelope of the $E_n(\phi)$ curves of individual many-body states $|n\rangle$. We will show that this quantity is related to the superfluid weight D_s.

Let us consider a sample of size $l_x\times l_y$, with a periodic boundary condition applied to the y direction and a *twisted* boundary condition applied to the x direction, i.e., the wave function satisfies $\Psi(x+l_x)=e^{i\phi}\Psi(x)$. This is gauge equivalent to the problem where the wave functions obey periodic boundary conditions in both directions so that the sample forms a torus and there is a Bohm-Aharonov flux applied inside the torus. The vector potential associated with the flux is given by $A_x=\phi/l_x$. As the magnitude of the flux is varied, the energies of the many-body eigenstates are changed, so that level crossings occur. Figure 2 shows the variation of the lowest-lying many-body energy eigenvalues $E_n(\phi)$ vs ϕ for both a noninteracting 4- and 8-site one-dimensional lattice and 4×4 and 8×8 two-dimensional lattices, all at one-quarter filling. Here the flux ϕ, measured in units of hc/e, passes through the one-dimensional ring or two-dimensional cylinder. We denote by ϕ_c the critical flux at which the first-level crossing occurs. For the one-dimensional case, the size of ϕ_c appears to be essentially the same for the 4- and 8-site lattices. However, for the two-dimensional case, ϕ_c has clearly decreased in going from the 4×4 to an 8×8 lattice. In Fig. 3, we have plotted $\ln(\phi_c)$ vs $\ln(l)$ for a number of two-dimensional $l\times l$ lattices with l up to 3000. The solid line corresponds to $\phi_c\sim l^{-1}$.

The order of magnitude of ϕ_c can be estimated as follows. The change in the energy of a many-body eigenstate due to the presence of the flux is of the order of $\Delta E\approx l^d A_x^2=l^{d-2}\phi^2$, where d is the dimension of the space, while the typical level spacing δE of the many-body eigenstates varies as $1/l^d$. This simple argument shows that the first-level crossing occurs at $\phi_c\approx 1/l^{(d-1)}$ (Ref. 19). Thus, in one dimension, ϕ_c approaches a finite value in the infinite volume limit, and there is no ambiguity in calculating its curvature at $\phi=0$. In this case one can follow the ground-state energy level adiabatically

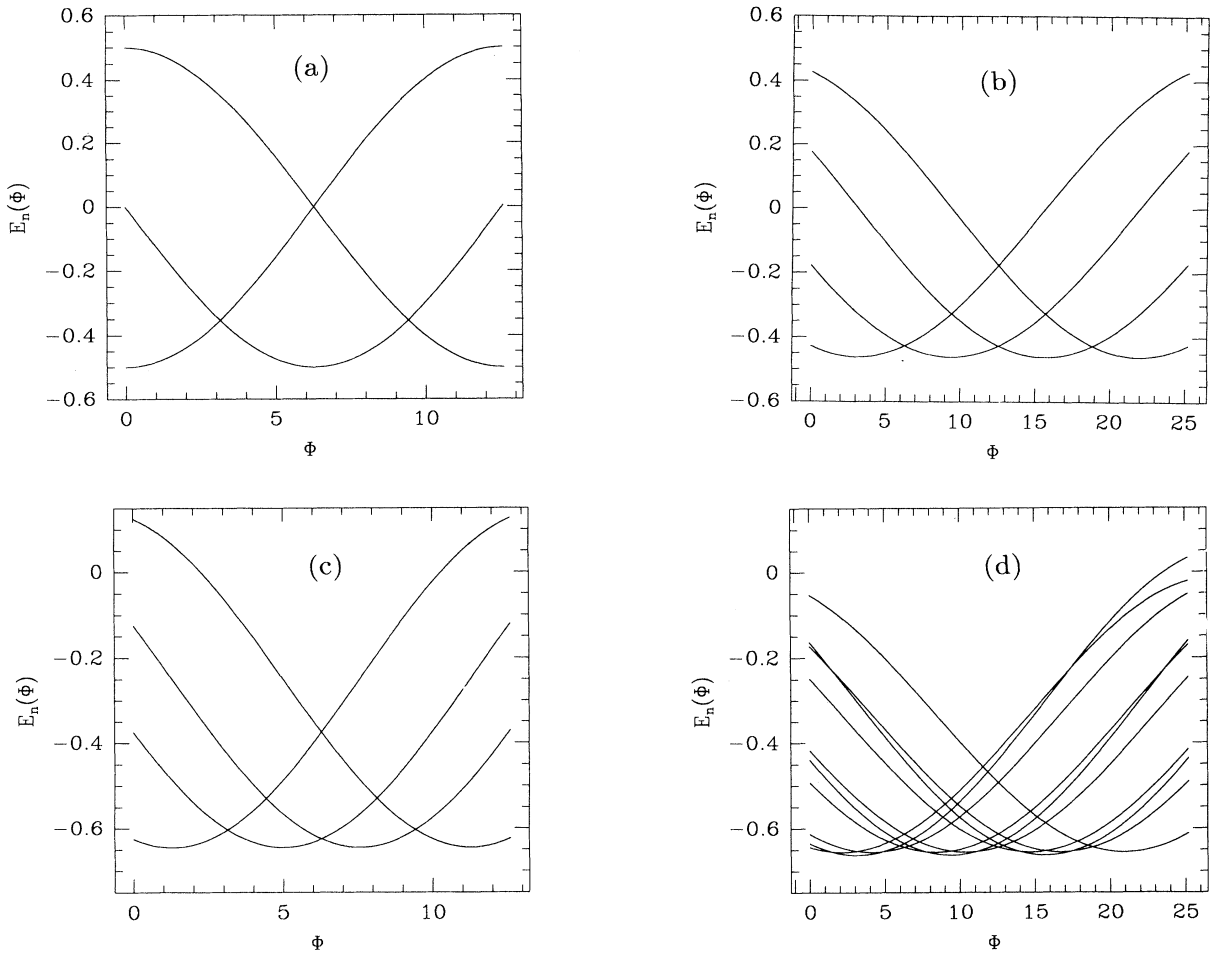

FIG. 2. Comparison of crossings of low-lying many-body energy levels $E_n(\phi)$ vs ϕ for one- and two-dimensional noninteracting spinless, quarter-filled systems: (a) one-dimensional 4-site lattice, (b) one-dimensional 8-site lattice, (c) two-dimensional 4×4 lattice, (d) two-dimensional 8×8 lattice. Here the flux ϕ is measured in units of hc/e.

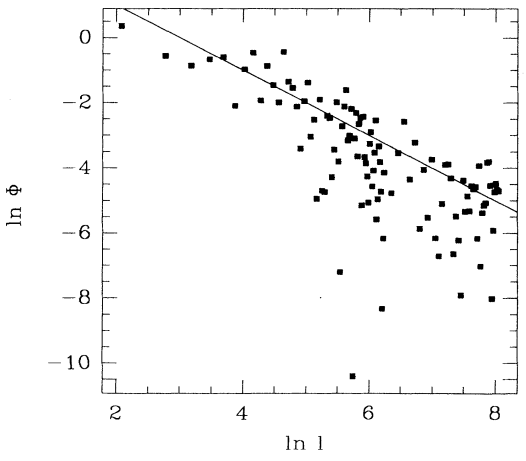

FIG. 3. Plot of $\ln(\phi_c)$ vs $\ln(l)$ for a two-dimensional $l\times l$ lattice which is one-quarter filled with spinless noninteracting electrons. Here ϕ_c is the flux at which the first many-body energy-level crossing occurs. Various values of l up to 3000 were examined. The solid line corresponds to $\phi_c \sim l^{-1}$.

as the flux is varied, obtaining the charge stiffness or Drude weight. However, in higher dimension, ϕ_c vanishes in the infinite volume limit, and in this limit the ground-state energy versus flux curve $E(\phi)$ is given by the *envelope* of the $E_n(\phi)$ curves of individual many-body states $|n\rangle$. Thus in $d>1$, there is a difference between calculating $\partial^2 E/\partial\phi^2$ for a finite system and then taking the limit $l\to\infty$ and calculating the $l\to\infty$ limit of $E(\phi)$ first and then determining the curvature. Kohn's formula relating $\partial^2 E/\partial\phi^2$ to the Drude weight D is based on the assumption that one may follow individual many-body energy levels adiabatically as one varies the flux, and calculate $\partial^2 E/\partial\phi^2$ perturbatively. However, for $d>1$ this would require that one calculate $\partial^2 E/\partial\phi^2$ for finite-sized lattices and then take the infinite volume limit. However, it is not clear that this procedure necessarily converges.

In the other limit, one first takes the thermodynamic limit of $E(\phi)$ while keeping the vector potential finite and then calculates $\partial^2 E/\partial\phi^2$. In this case, the typical level spacing δE is far less than the change in energy ΔE caused by the vector potential A_x. Therefore the contributions from the levels are averaged and the envelope

function $E(\phi)$ is obtained. This can be accomplished by considering our sample (with size $l_x \times l_y$) as a "unit cell" embedded in a larger "crystal" of size $L_x \times L_y$. The allowed values of the momenta are $p_x = 2\pi N_x / L_x$ and $p_y = 2\pi N_y / L_y$, and the level spacing is of the order of $1/L_x L_y$. The vector potential is applied uniformly over the sample, i.e., it is given by $A_x(x,y) = \phi_x / l_x$ if (x,y) is inside the sample and zero elsewhere. In the regime where $L \gg l$, one sees that the energy shift ΔE caused by A_x is indeed larger than the level spacing, therefore, to obtain the desired result one must take the $L \to \infty$ limit *before* one takes the $l \to \infty$ limit.

In the presence of the vector potential, the diamagnetic contribution to the energy shift is given by

$$\frac{\partial^2 E^{(1)}}{\partial A_x^2} = e^2 \langle k_x \rangle l_x l_y \ . \tag{30}$$

Here $l_x l_y$ is the area of the sample. The paramagnetic contribution to the energy shift is

$$\frac{\partial^2 E^{(2)}}{\partial A_x^2} = \sum_{q_x, q_y} |f(q_x)|^2 |f(q_y)|^2 \lim_{i\omega_m \to 0} L_x L_y \times \int_0^\beta d\tau \, e^{i\omega_m \tau} \langle j_x(q,\tau) j_x(-q,0) \rangle \ . \tag{31}$$

The form factor

$$f(q_x) = \frac{e^{iq_x l_x} - 1}{iq_x} \tag{32}$$

reflects the fact that $A_x(x,y)$ vanishes outside the sample, and $j_x(q)$ is the Fourier transform of the current density:

$$j_x(q) = \frac{1}{L_x L_y} \int_0^{L_x} dx \int_0^{L_y} dy \, e^{i(q_x x + q_y y)} j_x(x,y) \ . \tag{33}$$

As discussed above, the thermodynamic limit corresponds to taking the $L_x, L_y \to \infty$ *before* taking the $l_x, l_y \to \infty$ limit. Thus we set

$$\Lambda_{xx}(q) = \lim_{i\omega_m \to 0} \lim_{L_x, L_y \to \infty} L_x L_y \times \int_0^\beta d\tau \, e^{i\omega_m \tau} \langle j_x(q,\tau) j_x(-q,0) \rangle \ . \tag{34}$$

Then noting the fact that

$$\lim_{l_x \to \infty} \frac{1}{l_x} |f(q_x)|^2 = 2\pi \delta(q_x) \ , \tag{35}$$

and similarly for $f(q_y)$, we conclude that there are two limits of interest when $l_x, l_y \to \infty$,

$$\lim_{l_x \to \infty} \lim_{l_y \to \infty} \frac{1}{l_x l_y} \frac{\partial^2 E^{(2)}}{\partial A_x^2} = \lim_{q_x \to 0} \lim_{q_y \to 0} \Lambda_{xx}(q_x, q_y) \tag{36}$$

and

$$\lim_{l_y \to \infty} \lim_{l_x \to \infty} \frac{1}{l_x l_y} \frac{\partial^2 E^{(2)}}{\partial A_x^2} = \lim_{q_y \to 0} \lim_{q_x \to 0} \Lambda_{xx}(q_x, q_y) \ . \tag{37}$$

As we have seen from our earlier discussions, gauge invariance requires that the first limit approach $-e^2 \langle k_x \rangle$, exactly canceling the diamagnetic contribution, while the second limit gives the relevant information about whether a system has a finite *superfluid density*. Therefore, for a bulk two- or three-dimensional system,

$$\lim_{l_y \to \infty} \lim_{l_x \to \infty} \frac{1}{l_x l_y} \frac{\partial^2 E}{\partial A_x^2} = \frac{D_s}{\pi} \ . \tag{38}$$

If D_s is finite, we see that infinite volume limit in (36) and (37) depend on the aspect ratio of the system, reflecting the long-ranged current-current correlation of a superfluid.[10,12] The result (38) is also in agreement with Byers and Yang,[20] who argued that a superconductor can be identified by the macroscopic barrier in free energy between different flux minima. Thus for $d > 1$, we conclude that the curvature of the infinite volume limit of the ground-state energy, given by Eq. (38), is a measure of the superfluid density D_s.

As discussed above, one can study the superfluid weight by measuring the energy density, Eq. (38). At finite temperature one has a term in the free-energy density:

$$\Delta f = \tfrac{1}{2} n_s \phi^2 \ . \tag{39}$$

This implies that if one were to carry out a Monte Carlo calculation of the thermal internal energy density with a phase twist ϕ boundary condition,

$$\Delta e = \Delta f - T \frac{\partial}{\partial T} (\Delta f) \ , \tag{40}$$

so that near T_c

$$\Delta e \simeq -\frac{T_c}{2} \frac{\partial n_s}{\partial T} \phi^2 \ . \tag{41}$$

In the bulk limit in two dimensions, $n_s(T)$ has a Kosterlitz-Thouless[21] jump at T_c leading to a strong signal in Δe vs T [Eq. (41)] that can be very useful in numerical simulations.[22]

V. A THEOREM RELATING D AND D_s

We see from the discussions of the previous sections that D and D_s measure different physical responses, and they are obtained by taking different limits of the current-current correlation function. These two quantities are not equal in general, as seen from the trivial example of the free-electron gas discussed in Sec. III. However, in the examples of the SDW state and the BCS state, they are identical, vanishing in the former case, and equal to minus the kinetic energy in the x direction in the latter case. It therefore seems to be an empirical fact that they are equal whenever there is a gap in the spectrum. In the following, we shall prove that this empirical observation can be made into a rigorous theorem.

The gauge-invariant current-current correlation function can be written in the following general form:

$$\Lambda_{ij}(\mathbf{q}, z) = f(q^2, z) \delta_{ij} - g(q^2, z) \frac{q_i q_j}{q^2} \ , \tag{42}$$

where the scalar functions $f(q^2,z)$ and $g(q^2,z)$ are obtained by analytically continuing the Matsubara frequencies $i\omega_m$ into the complex z plane. In general, these func-

tions are analytic everywhere except for a possible branch cut or isolated poles on the real axis. Gauge invariance requires that

$$\lim_{z\to 0} g(q^2,z)=\lim_{z\to 0} f(q^2,z)\ , \tag{43}$$

so that Λ_{ij} is purely transverse in the static limit. We define the existence of a gap in terms of the analytic properties of $f(q^2,z)$, so that for each q, there is a "gap" $\tilde{\Delta}_q$, such that the branch cut singularity of f vanishes for $|\omega|<\tilde{\Delta}_q$ (see Fig. 4), and this gap persists in the $q\to 0$ limit, i.e., $\lim_{q\to 0}\tilde{\Delta}_q\equiv\tilde{\Delta}_0\neq 0$. This property holds for an SDW insulator or an s-wave BCS superconductor, where $\tilde{\Delta}_0$ is twice the quasiparticle gap $2\Delta_0$. In a superconductor without long-range interactions, there is a gapless Goldstone mode in the longitudinal channel $g(q^2,z)$; however, this does not affect the analytical properties of $f(q^2,z)$. From the fact that

$$\mathrm{Im}f(q^2,\omega-i\eta)=(1/2i)[f(q^2,\omega+i\eta)-f(q^2,\omega-i\eta)]\ ,$$

it follows that

$$\lim_{\eta\to 0}\mathrm{Im}f(q^2,\omega-i\eta)=0 \tag{44}$$

for $|\omega|<\tilde{\Delta}_q$. From the Kramers-Kronig relation, we have

$$\mathrm{Re}f(q^2,\omega)=\frac{1}{\pi}P\int_{-\infty}^{\infty}\frac{\mathrm{Im}f(q^2,\varepsilon)}{\varepsilon-\omega}d\varepsilon\ . \tag{45}$$

From Eq. (44) it follows that this integral does not contain any singularities if $|\omega|<\tilde{\Delta}_q$. Combined with the fact that $\lim_{q\to 0}\tilde{\Delta}_q\equiv\tilde{\Delta}_0\neq 0$, we conclude that the $q\to 0$ and the $\omega\to 0$ limits of $f(q^2,\omega)$ are interchangeable,

$$\lim_{q\to 0}\lim_{\omega\to 0}f(q^2,\omega)=\lim_{\omega\to 0}\lim_{q\to 0}f(q^2,\omega)$$

$$=\frac{2}{\pi}\int_{\tilde{\Delta}_0}^{\infty}\frac{\mathrm{Im}f(0,\varepsilon)}{\varepsilon}d\varepsilon\ , \tag{46}$$

so that $D=D_s$ if there is a gap in the spectrum.

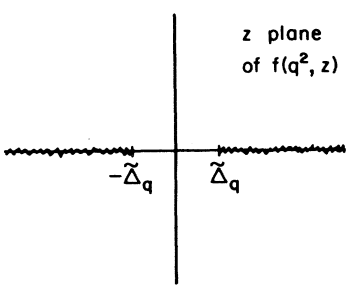

FIG. 4. Analytic structure of $f(q^2,z)$. For each q there is a gap $\tilde{\Delta}_q$, and the branch cut singularity stops at $\pm\tilde{\Delta}_q$ as shown.

VI. MONTE CARLO RESULTS

As discussed in the Introduction, our original interest in these questions arose from the desire to develop a calculational Monte Carlo procedure for determining whether a given interacting electron system was insulating, metallic, or superconducting. We have previously reported some of the results which were obtained from simulations carried out on both positive- and negative-U Hubbard models.[7] Here we discuss further numerical results for $\Lambda_{xx}(q,i\omega_m)$ and $\langle -k_x\rangle$ obtained for these systems.

The quantum Monte Carlo method we are using is a version of the grand-canonical exact-updating determinantal method developed by Blankenbecler, Scalapino, and Sugar.[23] It incorporates matrix factorization methods,[24,25] which are a generalization of the stabilization method developed by Sugiyama and Koonin[26] and used by Sorella *et al.*[27] The time-slice spacing $\Delta\tau$ has been set to 0.125 throughout, which gives systematic errors of a few percent. Typically, 5000 sweeps through the lattice were used. The Monte Carlo has been checked in a variety of ways, including detailed comparisons of various quantities with results from exact diagonalization of a 2×2 lattice. For $U>0$ at half-filling $\langle n\rangle=1$, there is no determinantal sign problem,[28] and it is straightforward to go to low temperatures. Here on a 10×10 lattice we will show results for $\beta=10$. However, for $U>0$, away from half-filling, the temperatures that could be reached were limited by the sign problem, to β of order 6 for an 8×8 lattice. Here, and in the following, we will measure energy in units of t. For a two-dimensional lattice, the bandwidth is $8t$, so that $\beta=10$ implies that kT is 1/80 of the bandwidth, while $\beta=6$ implies that kT is 1/48 of the bandwidth.

Although the evolution through configuration space is stabilized with matrix factorization techniques, the measurement of the Green's function used to determine the current-current correlation function was based on the expanded matrix method of Hirsch,[29] which is a generalization of the method of White, Sugar and Scalettar.[30] Al-

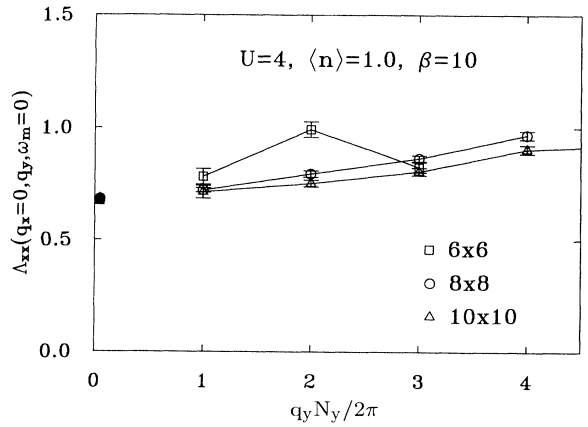

FIG. 5. Monte Carlo results for $\Lambda_{xx}(q_x=0,\ q_y,\ \omega_m=0)$ vs q_y for $U=4$, $\langle n\rangle=1$, and $\beta=10$ on various sized lattices. The solid symbols denote $\langle -k_x\rangle$.

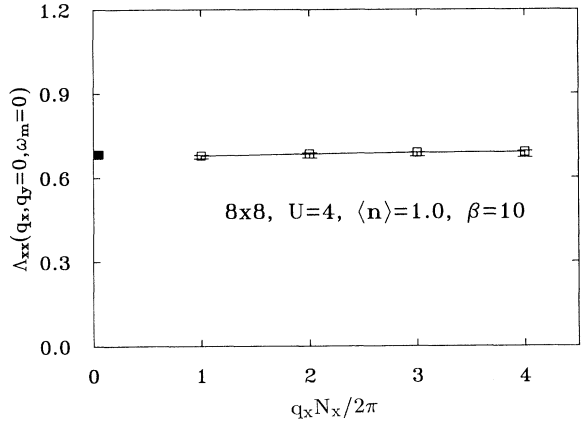

FIG. 6. $\Lambda_{xx}(q_x,q_y=0,\omega_m=0)$ vs q_x for $U=4$, $\langle n\rangle=1$, and $\beta=10$ on an 8×8 lattice. The solid symbol is $\langle -k_x\rangle$.

though slower than the matrix factorization methods for the Monte Carlo evolution, this method gives results for all τ and τ' in one calculation, rather than giving results for all τ for fixed τ', as the factorization method does. The redundant information (since the exact result for the Green's function depends only on $\tau-\tau'$) is used to help reduce the statistical errors, and we have found that this makes the expanded matrix method more efficient for calculating time-dependent observables.

In Fig. 5, Monte Carlo results for $\Lambda_{xx}(q_x=0,q_y,\omega_m=0)$ vs q_y are shown for the half-filled $\langle n\rangle=1$ Hubbard model with $U=4$ at an inverse temperature $\beta=10$. At this low temperature, relative to $J\simeq4t^2/U=1$, the antiferromagnetic correlation length is greater than the linear dimension of the largest lattice shown. As the lattice size increases from 6×6 to 10×10, we see that $\Lambda_{xx}(q_x=0,q_y\to0,\omega_m=0)$ tends towards $\langle -k_x\rangle$, shown as the solid symbol. Thus, as expected, there is no superfluid density in the half-filled Hubbard model with $U=4$. Gauge invariance, which requires that $\Lambda(q_x\to0,q_y=0,\omega_m=0)=\langle -k_x\rangle$, is clearly seen in

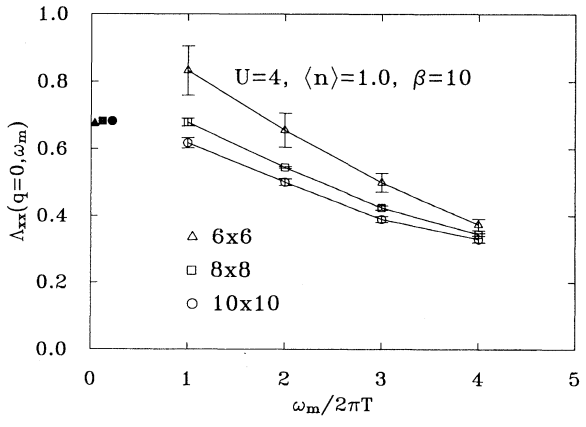

FIG. 7. $\Lambda_{xx}(q=0,\omega_m)$ vs ω_m for $U=4$, $\langle n\rangle=1$, and $\beta=10$ on 6×6(△), 8×8(□), and 10×10(○) lattices. The solid symbols denote the values of $\langle -k_x\rangle$.

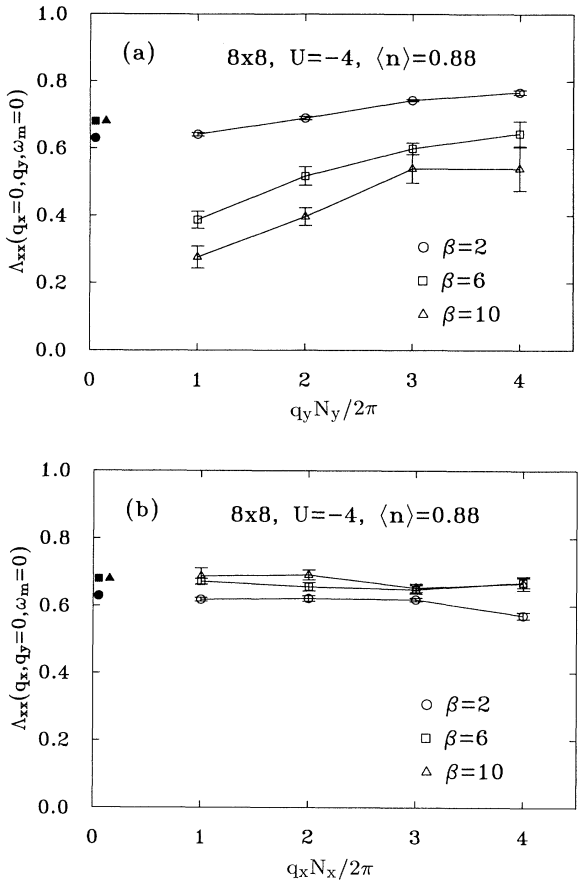

FIG. 8. Monte Carlo results for the attractive Hubbard model, (a) $\Lambda_{xx}(q_x=0,q_y,\omega_m=0)$ vs q_y, and (b) $\Lambda_{xx}(q_x,q_y=0,\omega_m=0)$ vs q_x for $U=-4$, $\langle n\rangle=0.875$, and $\beta=2$, 6, and 10. The solid symbols denote $\langle -k_x\rangle$.

Fig. 6.

Next we examine in Fig. 7 the $\mathbf{q}=\mathbf{0}$, $\omega_m\to0$ limit for the same set of lattices as shown in Fig. 5. In this case there is also a clear indication that as the size of the lattice increases, $\Lambda_{xx}(\mathbf{q}=0,\omega_m\to0)$ converges towards

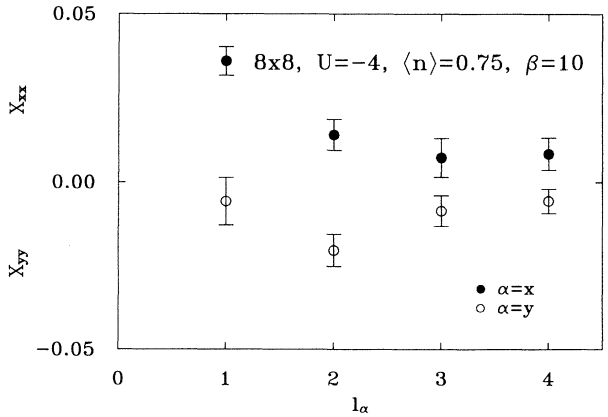

FIG. 9. The static current-current correlation function $\chi_{xx}(l_x,0)$ vs l_x (solid points) and $\chi_{xx}(0,l_y)$ vs l_y (open points) for $U=-4$ with $\langle n\rangle=0.75$ and $\beta=10$.

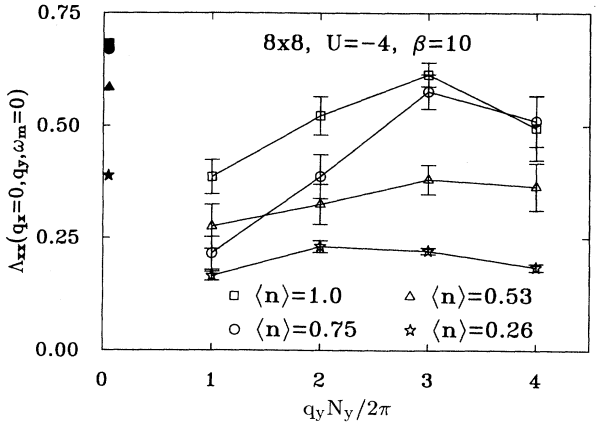

FIG. 10. $\Lambda_{xx}(q_x=0, q_y, \omega_m=0)$ vs q_y for an 8×8 lattice with $U=-4$, $\beta=10$, and different fillings. As usual, the solid symbols denote $\langle -k_x \rangle$.

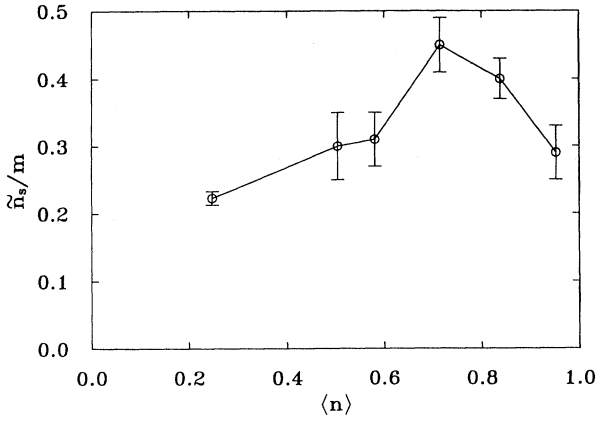

FIG. 11. $(\bar{n}_s/m)=\langle -k_x \rangle - \Lambda_{xx}(q_y=\pi/4, \omega_m=0)$ vs the filling $\langle n \rangle$ for $U=-4$ and $\beta=10$ obtained from an 8×8 lattice.

$\langle -k_x \rangle$, implying a vanishing Drude weight. Thus we find that the half-filled Hubbard model with $U=4$ has $D=D_s=0$ and is insulating. On the smaller lattices, it appears that $\Lambda_{xx}(\mathbf{q}=0, \omega_m \to 0)$ converges to a value greater than $\langle -k_x \rangle$, implying a negative "paramagnetic" Drude weight on these finite clusters. Previous work on one-dimensional Hubbard rings[16,17] showed that for half-filled rings with $4n$ sites, D was negative, while for rings with $4n+2$ sites, D was positive. In both these cases, the magnitude of D vanished exponentially with

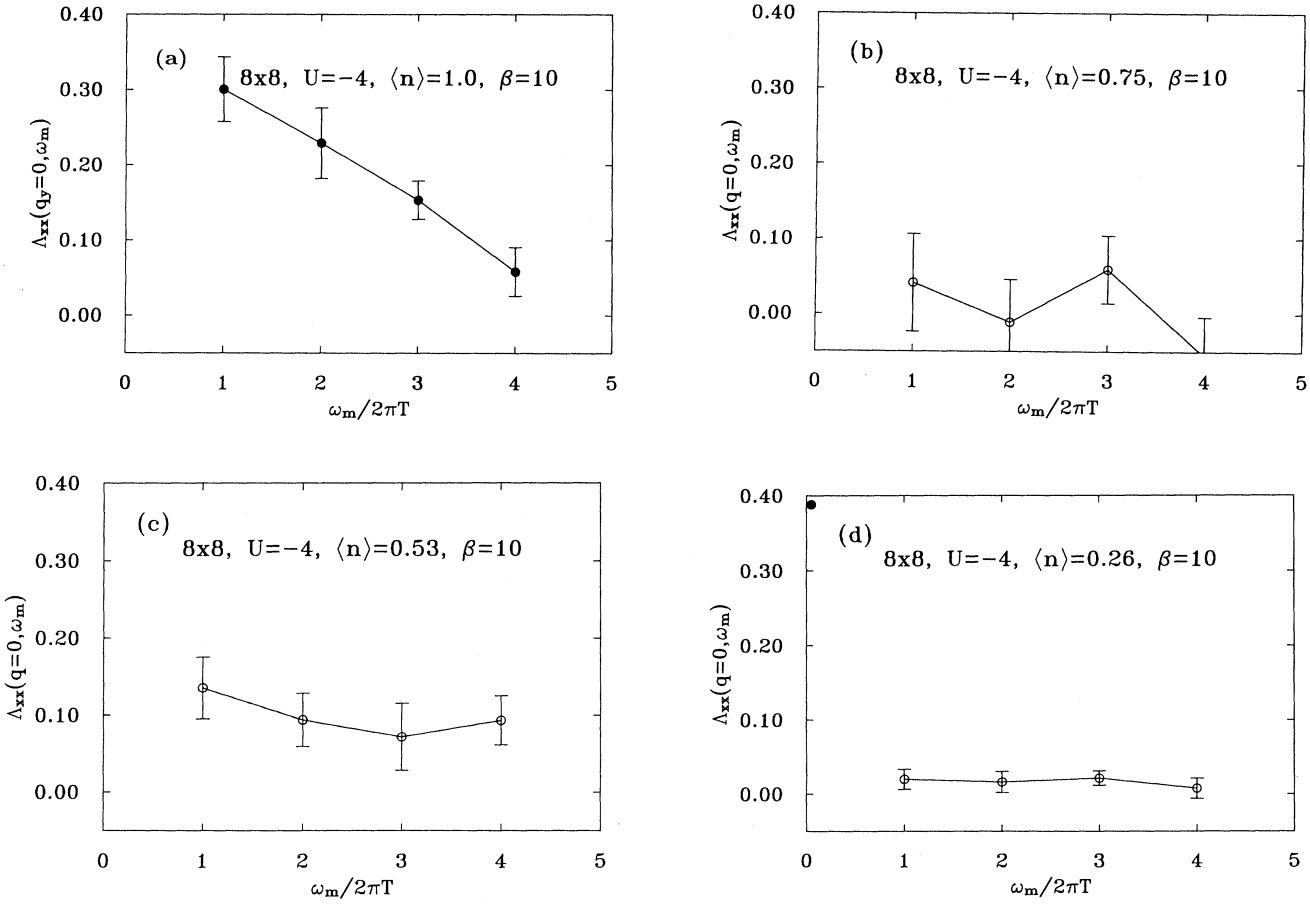

FIG. 12. $\Lambda_{xx}(\mathbf{q}=\mathbf{0}, \omega_m)$ vs ω_m for $U=-4$, $\beta=10$ on an 8×8 lattice for the same band fillings $\langle n \rangle$ as Fig. 10.

the number of sites in the ring.

Turning next to the negative-U Hubbard model, we have calculated Λ_{xx} on an 8×8 lattice with $U=-4$ at different temperatures and fillings. Results showing $\Lambda_{xx}(q_y,\omega_m=0)$ vs q_y for various temperatures at a filling of $\langle n\rangle=0.875$ are plotted in Fig. 8(a). As before, half the kinetic energy per site $\langle -k_x\rangle$ is shown as the solid symbols. At high temperatures, $\beta=2$, $\Lambda_{xx}(q_y\to0,\omega_m=0)$ extrapolates towards $\langle -k_x\rangle$ and the superfluid density vanishes. As the system is cooled, $\beta=6$ and $\beta=10$, the $\Lambda_{xx}(q_y,\omega_m=0)$ response decreases below $\langle -k_x\rangle$, implying a nonvanishing value of D_s and hence a finite superfluid density. The longitudinal response $\Lambda_{xx}(q_x\to0,\ q_y=0,\omega_m=0)$ for the same parameters is shown versus q_x in Fig. 8(b). It approaches $\langle -k_x\rangle$ as required by gauge invariance.

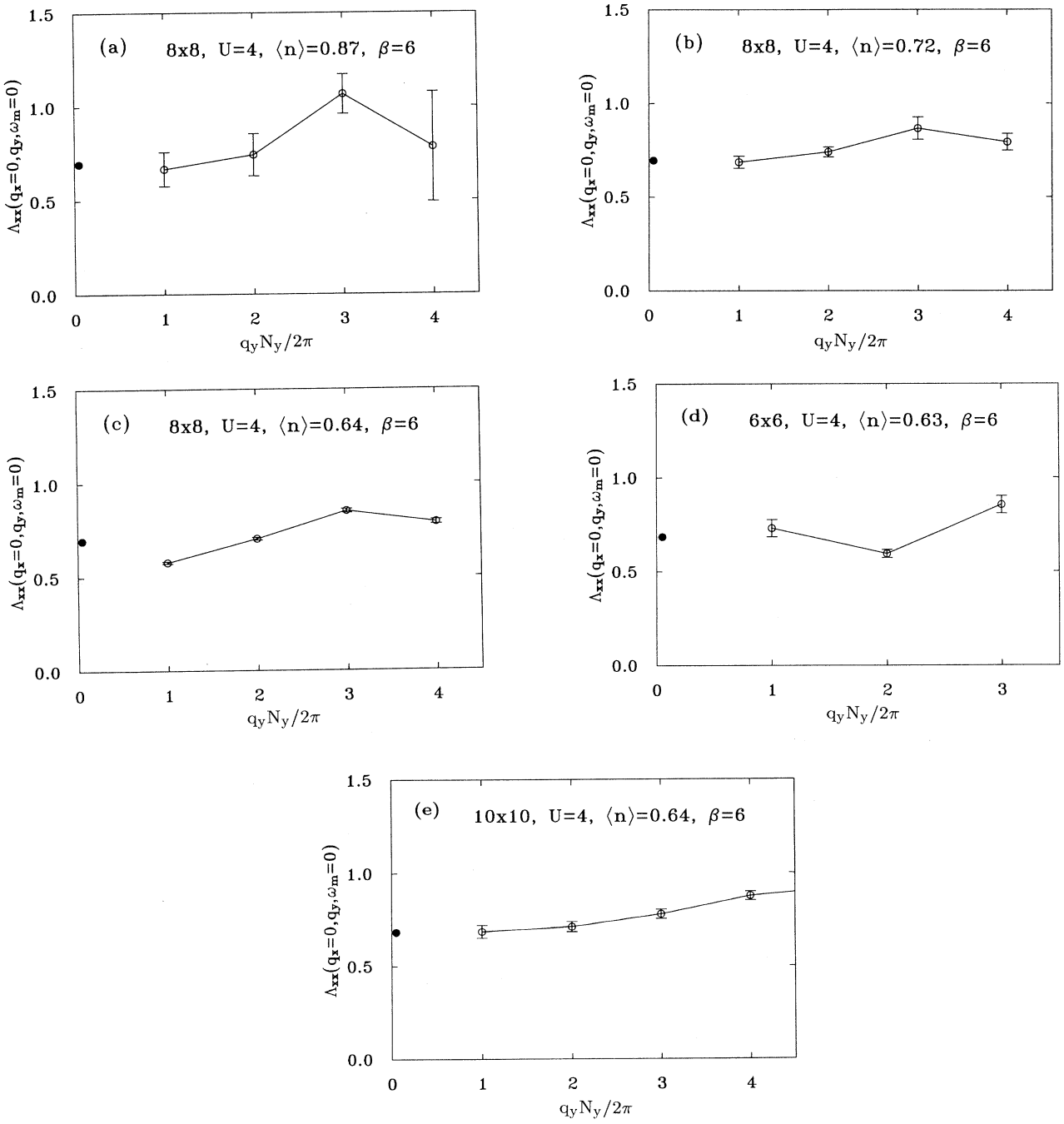

FIG. 13. $\Lambda_{xx}(q_x=0,\ q_y,\ \omega_m=0)$ vs q_y for an 8×8 lattice with $U=4$, $\beta=6$, and various band fillings: (a) $\langle n\rangle=0.87$, (b) $\langle n\rangle=0.72$, and (c) $\langle n\rangle=0.64$. The solid symbol is $\langle -k_x\rangle$. (d) and (e) show $\Lambda_{xx}(q_x=0,\ q_y,\ \omega_m=0)$ for essentially the same filling as (c) on 6×6 and 10×10 lattices respectively. In this parameter range at $\beta=6$ we conclude D_s vanishes.

As noted in Sec. II, the fact that $\Lambda_{xx}(q_x,q_y,\omega_m=0)$ approaches different limiting values depending upon the order in which q_x and q_y are taken to zero implies the existence of long-range, power-law, current-current correlations. This is characteristic of the super-conducting state and arises from the macroscopic occupation of the center-of-mass wave functions of the pairs. In the superconducting state, the spatial dependence of the static current-density correlation function

$$\chi_{xx}(l_x,l_y)=\frac{1}{N}\sum_q e^{i(q_x l_x+q_y l_y)} \times\int_0^\beta d\tau\langle j_x(q,\tau)j_x(-q,0)\rangle \quad (47)$$

is expected to vary as $(l_x-l_y)/(2\pi)(l_x^2+l_y^2)^{3/2}$. In Fig. 9, results for $\chi_{xx}(l_x,l_y)$ vs l_x and l_y are shown for $U=-4$, $\langle n\rangle=0.75$, and $\beta=10$. Here $\chi_{xx}(l_x,0)$ vs l_x is plotted as the solid points and $\chi_{xx}(0,l_y)$ vs l_y as the open points. Note that out along the l_x axis, the j_x-j_x correlation is positive, while out along the l_y axis the j_x-j_x correlation is negative, as would be expected for a dipolar backflow pattern. This dipole backflow is characteristic of the superconducting state.

Results showing $\Lambda_{xx}(q_y,\omega_m=0)$ vs q_y at various fillings calculated for an 8×8 lattice with $U=-4$ and $\beta=10$ are shown in Fig. 10. In Fig. 11 we have used the value of $\Lambda_{xx}(q_y,\omega_m=0)$ at the smallest $q_y=\pi/4$ momentum available on an 8×8 lattice to provide as estimate of $(\tilde{n}_s/m)$ vs the filling $\langle n\rangle$:

$$\left[\frac{\tilde{n}_s}{m}\right]\simeq\langle -k_x\rangle-\Lambda_{xx}\left[q_y=\frac{\pi}{4},\omega_m=0\right]. \quad (48)$$

The value of $(\tilde{n}_s/m)$ obtained in this manner first increases as $\langle n\rangle$ is doped away from half-filling and then decreases. On general grounds, one expects that for $\langle n\rangle\neq1$, the two-dimensional negative-U Hubbard model will exhibit a finite temperature Kosterlitz-Thouless[21] transition to a state with a nonvanishing superfluid density. At half-filling, $\langle n\rangle=1$, this transition temperature goes to zero, and the ground state has both long-range charge-density-wave and pair-field correlations.[31,32]

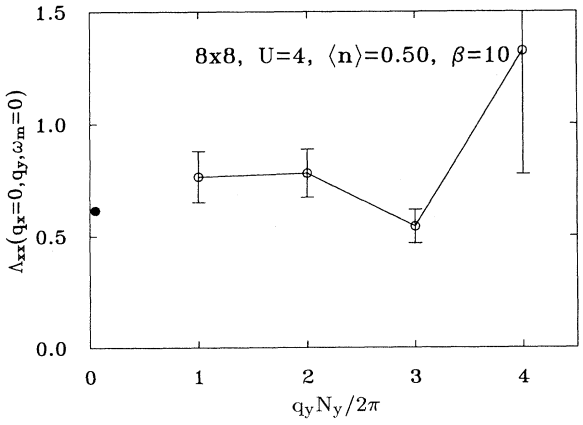

FIG. 14. $\Lambda_{xx}(q_x=0,\ q_y,\ \omega_m=0)$ vs q_y on an 8×8 lattice with $U=4$, $\beta=10$, and $\langle n\rangle=0.5$.

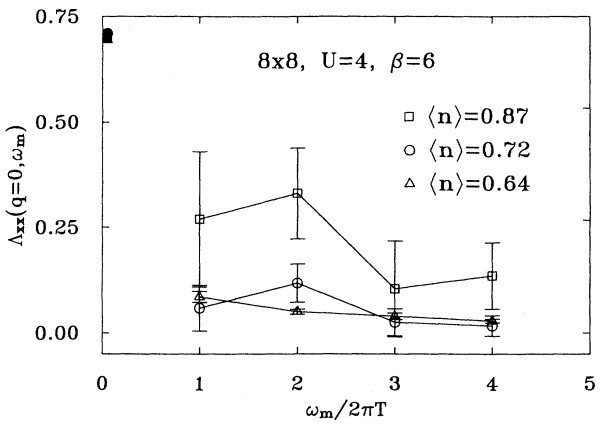

FIG. 15. $\Lambda_{xx}(\mathbf{q}=\mathbf{0},\ \omega_m)$ vs ω_m for an 8×8 lattice with $U=4$, $\beta=6$, and the same band fillings as Fig. 13.

These expectations are consistent with the behavior shown in Figs. 10 and 11. The dependence of $\Lambda_{xx}(\mathbf{q}=\mathbf{0},\ \omega_m)$ on ω_m for $U=-4$ and $\beta=10$ is shown in Fig. 12. This clearly shows that $D/\pi e^2$ is finite, so the system has zero resistance.

Finally, we consider the repulsive-U Hubbard model when it is doped away from half-filling. In this case, as is well known,[28] the fermion determinant is not positive definite, and its average sign vanishes exponentially with increasing β. This limits the maximum value of β that can be reached. Here we will examine results for $\Lambda_{xx}(\mathbf{q},i\omega_m)$ obtained from simulations of an 8×8 lattice with $U=4$ and $\beta=6$. Figure 13 shows $\Lambda_{xx}(q_y,\omega_m=0)$ vs q_y for various band fillings $\langle n\rangle$. The determinantal sign problem is particularly severe for $\langle n\rangle=0.87$, as seen by the error bars in Fig. 13(a). We also show in Fig. 14 results for $\Lambda_{xx}(q_y,\omega_m=0)$ vs q_y, with $\langle n\rangle=0.5$ at $\beta=10$. With the exception of Fig. 13(c) for $\langle n\rangle=0.64$, we conclude that in this parameter range D_s appears to vanish for the non-half-filled two-dimensional Hubbard model. A possible explanation of the $\langle n\rangle=0.64$ results shown in Fig. 13(c) is that it is a finite-size effect. In Figs. 13(d) and 13(e) we show $\Lambda_{xx}(q_y,\omega_m=0)$ for 6×6 and 10×10 lattices at this filling and indeed find that this is the case.

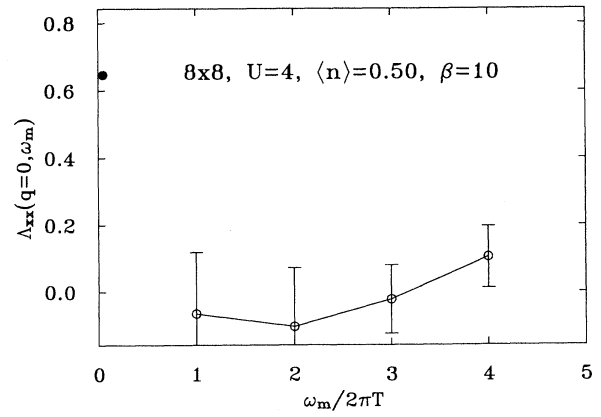

FIG. 16. $\Lambda_{xx}(\mathbf{q}=\mathbf{0},\ \omega_m)$ vs ω_m for an 8×8 lattice with $U=4$, $\beta=10$, and $\langle n\rangle=0.5$. The solid symbol shows $\langle -k_x\rangle$.

In Fig. 15, the variation of $\Lambda_{xx}(\mathbf{q}=\mathbf{0}, \omega_m)$ with ω_m is plotted for the same set of fillings and temperature $\beta=6$ as used in Fig. 13. Results for $\langle n \rangle = 0.5$ and $\beta=10$ are shown in Fig. 16. It would appear from these results that the positive-U Hubbard model doped away from half-filling has a finite Drude weight. Thus data from the temperature regime accessible to the simulation suggest that the non-half-filled two-dimensional Hubbard model is a metal but not a superconductor.

VII. CONCLUSION

In this paper we have shown that the limiting behavior of the current-current correlation function provides criteria for determining whether a system is insulating, metallic, or superconducting. Based upon these criteria, we have presented numerical evidence that the ground state of the half-filled repulsive-U Hubbard model is an insulator, the negative-U Hubbard model is a superconductor, and within the parameter regime accessible to our simulations, the non-half-filled Hubbard model appears to be metallic but not superconducting.

Here we conclude with some general comments. We believe that the limiting $\mathbf{q}\rightarrow\mathbf{0}$ and $\omega\rightarrow 0$ behaviors of the current-current correlation function [Eqs. (15) and (22)] provide useful conceptual and numerical criteria for determining whether a system is insulating, metallic, or superconducting. However, in one dimension, there is just the Drude weight [Eq. (22)] since one cannot put on a transverse vector potential. As noted, for a one-dimensional system, ϕ_c is some fraction of hc/e and does not decrease as the length l of the system increases. Thus, for various one-dimensional systems, $\partial^2 E_0/\partial\phi^2|_{\phi=0}$ also provides a useful way of calculating the Drude weight or charge stiffness. In particular, D is finite for the one-dimensional, half-filled positive-U Hubbard model. However, the dominant power-law decay of correlations occurs in the $2p_F$ spin-density wave channel, and this system is clearly metallic rather than a paired superconducting state. In this case, one can examine the functional behavior of $E_0(\phi)$. As discussed by Yang and Byers, when there is pairing, $E_0(\phi)$ will be periodic with a period $hc/2e$. In practice it is important to examine the scaling properties of $E_0(\phi)$. For a nonsuperconducting ground state, one expects $E_0(\phi=\pi)-E_0(\phi=0) \approx N_e/l^2$ with N_e the number of electrons, whereas for a superconducting ground state $E_0(\phi=\pi)-E_0(\phi=0) \approx 1/l^2$. Alternatively, one can examine the behavior of the Drude weight when impurities are introduced.[33]

Finally, a comment regarding the nonzero value of D which we found for the 8×8 non-half-filled positive-U Hubbard model at the end of the last section is in order. This nonzero value for D was obtained for a finite 8×8 lattice at a temperature below the threshold for quasiparticle-hole excitation on such a discrete system. If the temperature is held fixed at $\beta=6$ and the lattice size increased, $\Lambda_{xx}(q=0, \omega_m\rightarrow 0)$ will approach $\langle -k_x \rangle$ and D will vanish when the low-lying quasiparticle-hole excitations have energies less than kT. Thus as the lattice size increases, we expect that the temperature threshold below which D is finite scales to zero so that for a normal metal with an infinite lattice, D vanishes unless $T=0$.

ACKNOWLEDGMENTS

We thank E. Dagotto, A. Millis, M. Fisher, R. T. Scalettar, and J. R. Schrieffer for useful discussions. We would also like to thank A. Sandvik for the calculations shown in Figs. 2 and 3. D.J.S. would like to thank IBM Research and the Almaden Laboratory, and the Correlated Electron Theory Program at the Center for Materials Science, Los Alamos National Laboratory, for their support and hospitality; the Department of Energy for support under Grant No. DE-FG03-85ER45197; and the Electric Power Research Institute under Grant No. RP8009-18. S.R.W. would like to thank the Office of Naval Research for support under Grant No. N00014-91-J-1143. This research was also supported in part by the University of California through an allocation of computer time (S.R.W.) and by NERSC (D.J.S.).

[1] D. J. Scalapino, in *High Temperature Superconductivity Proceedings*, edited by K. S. Bedell, D. Coffey, D. E. Meltzer, D. Pines, and J. R. Schrieffer (Addison-Wesley, Reading, MA, 1990), p. 314.
[2] J. E. Hirsch and S. Tang, Phys. Rev. Lett. **62**, 591 (1989).
[3] S. R. White, D. J. Scalapino, R. L. Sugar, E. Y. Loh, J. E. Gubernatis, and R. T. Scalettar, Phys. Rev. B **40**, 506 (1989).
[4] A. Moreo and D. J. Scalapino, Phys. Rev. B **43**, 8211 (1991).
[5] M. Imada and Y. Hatsugai, J. Phys. Soc. Jpn. **58**, 3752 (1989); N. Furukawa and M. Imada, Physica C **185–189**, 1443 (1991).
[6] E. Dagotto and J. R. Schrieffer, Phys. Rev. B **43**, 8705 (1991).
[7] D. J. Scalapino, S. R. White, and S. C. Zhang, Phys. Rev. Lett. **68**, 2830 (1992).
[8] R. E. Peierls, Z. Phys. **80**, 763 (1933).
[9] J. R. Schrieffer, *Theory of Superconductivity* (Addison-Wesley, Reading, MA, 1964), pp. 203–253.
[10] D. Pines and P. Nozieres, *The Theory of Quantum Liquids I* (Addison-Wesley, Reading, MA, 1966), pp. 148–200.
[11] F. London, *Superfluids* (Wiley, New York, 1950), Vol. I, pp. 27–95.
[12] D. Forster, *Hydrodynamic Fluctuations, Broken Symmetry, and Correlation Functions* (Benjamin, New York, 1975), pp. 214–223.
[13] W. Kohn, Phys. Rev. **133**, A171 (1964).
[14] B. Shastry and B. Sutherland, Phys. Rev. Lett. **65**, 243 (1990).
[15] In this case $(n_s/m)^* = -\langle k_x \rangle$, which varies as t in weak coupling and $t^2/|U|$ in strong coupling, J. E. Hirsch and F. Marsiglio (unpublished).
[16] R. M. Fye *et al.*, Phys. Rev. B **44**, 6909 (1991); E. Dagotto *et al.* (unpublished).
[17] C. Stafford, A. Millis, and B. Shastry, Phys. Rev. B **43**, 13 660 (1991).
[18] D. Poilblanc, Phys. Rev. B (to be published).
[19] Shastry and Sutherland (Ref. 14) argue that $\phi_c \approx 1/l^{(d-1)/2}$, which differs from our estimation but still has the property that ϕ_c vanishes in the infinite volume limit for $d>1$.

[20]N. Byers and C. N. Yang, Phys. Rev. Lett. **7**, 46 (1961).
[21]J. M. Kosterlitz and D. J. Thouless, J. Phys. C **6**, 1181 (1973).
[22]E. Loh, Jr., D. J. Scalapino, and P. M. Grant, Phys. Rev. B **31**, 4712 (1985); Phys. Scr. **32**, 327 (1985). In these papers, the phase diagrams of the $s=1/2$ quantum xy and xxz models were studied by calculating $E(T,\phi=\pi)-E(T,\phi=0)$.
[23]R. Blankenbecler, D. J. Scalapino, and R. L. Sugar, Phys. Rev. D **24**, 2278 (1981).
[24]S. R. White, D. J. Scalapino, R. L. Sugar, E. Y. Loh, J. E. Gubernatis, and R. T. Scalettar, Phys. Rev. B **40**, 506 (1989).
[25]E. Y. Loh, J. E. Gubernatis, R. T. Scalettar, R. L. Sugar, and S. R. White, in *Interacting Electrons in Reduced Dimensions,* edited by D. Baeriswyl and D. Campbell (Plenum, New York, 1989), pp. 55–60.
[26]G. Sugiyama and S. E. Koonin, Ann. Phys. (N.Y.) **168**, 1 (1986).
[27]S. Sorella, S. Baroni, R. Car, and M. Parrinello, Europhys. Lett. **8**, 663 (1989); S. Sorella, E. Tosatti, S. Baroni, R. Car, and M. Parrinello, Int. J. Mod. Phys. B **1**, 993 (1989).
[28]E. Y. Loh, J. E. Gubernatis, R. T. Scalettar, S. R. White, D. J. Scalapino, and R. L. Sugar, Phys. Rev. B **41**, 9301 (1990).
[29]J. E. Hirsch, Phys. Rev. B **38**, 12 023 (1988).
[30]S. R. White, R. L. Sugar, and R. T. Scalettar, Phys. Rev. B **38**, 11 665 (1988).
[31]R. T. Scalettar *et al.*, Phys. Rev. Lett. **62**, 1407 (1989).
[32]A. Moreo and D. J. Scalapino, Phys. Rev. Lett. **66**, 946 (1991).
[33]The role of disorder in one-dimensional interacting Bose systems has been recently studied using quantum Monte Carlo techniques by R. T. Scalettar, G. G. Batrouni, and G. T. Zimanyi, Phys. Rev. Lett. **66**, 3144 (1991).